Electronic Supplementary Material (ESI) for Dalton Transactions.

Supporting Information

Low Volume Expansion Hierarchical Porous Sulfur-Doped Fe_2O_3@C with High-Rate Capability for Superior Lithium Storage

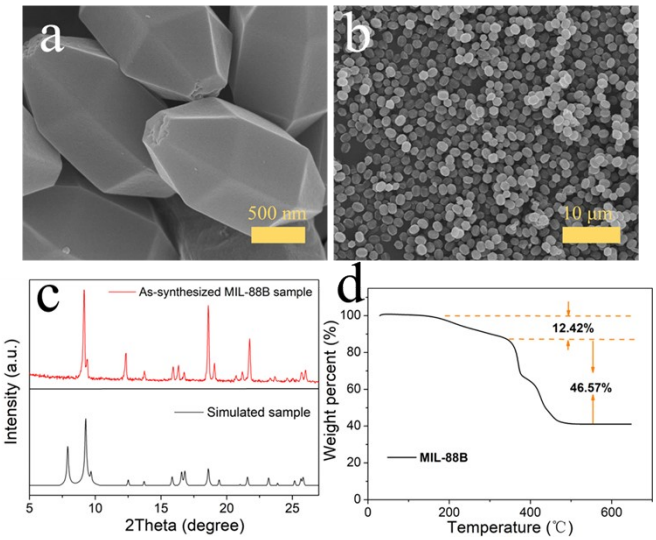

Figure S1. (a, b) SEM images, (c) XRD patterns, and (d) TG curve of MIL-88B NSs

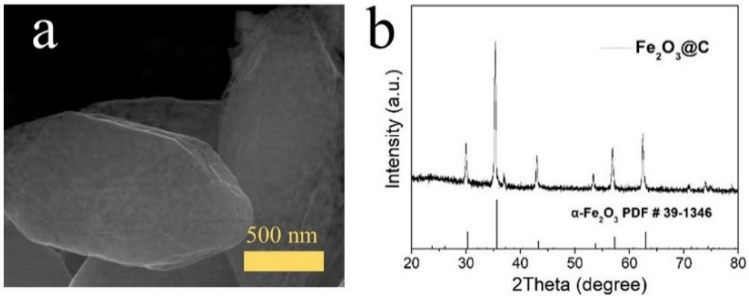

Figure S2. (a) SEM image and (b) XRD pattern of Fe_2O_3@C NSs

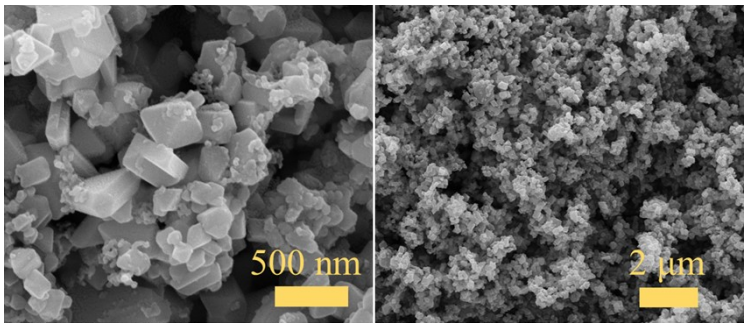

Figure S3. (a, b) SEM images of Fe_2O_3/C NSs

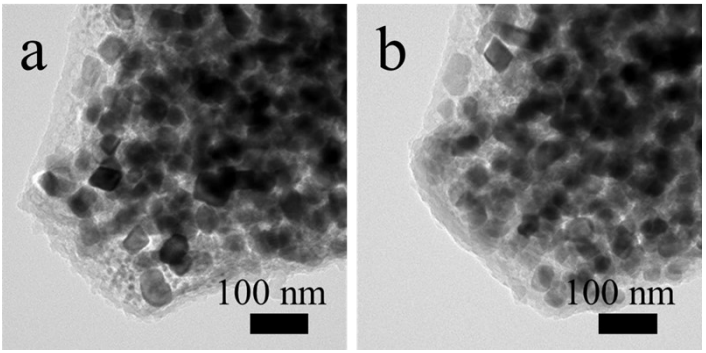

Figure S4. TEM images of (a) S_0-Fe_2O_3@C and (b) $S_{0.15}$-Fe_2O_3@C NSs

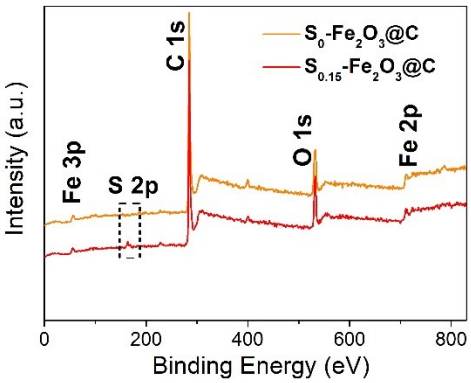

Figure S5. XPS survey spectra of S_0-Fe_2O_3@C and (b) $S_{0.15}$-Fe_2O_3@C NSs

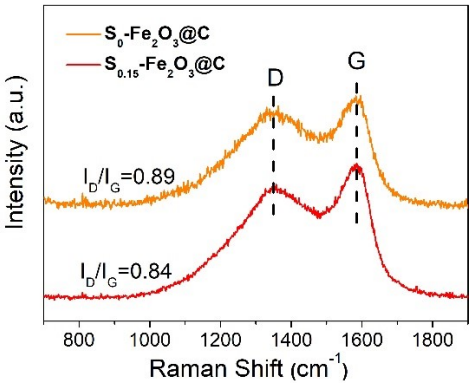

Figure S6. Raman spectra of S_0-Fe_2O_3@C and $S_{0.15}$-Fe_2O_3@C NSs

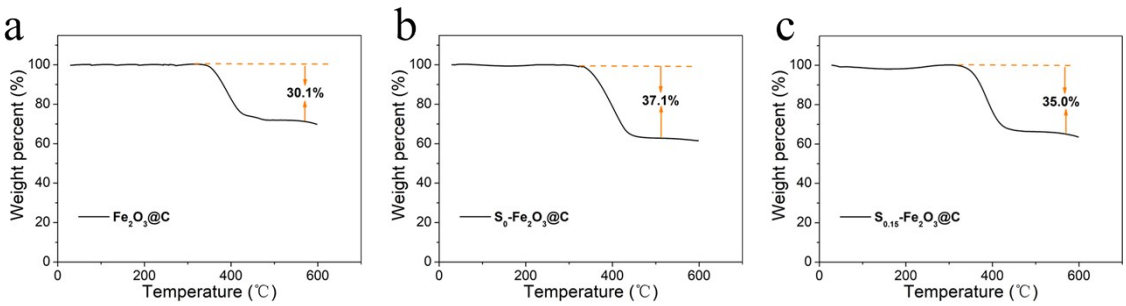

Figure S7. TG curves of (a) Fe_2O_3@C, (b) S_0-Fe_2O_3@C, and (c) $S_{0.15}$-Fe_2O_3@C NSs

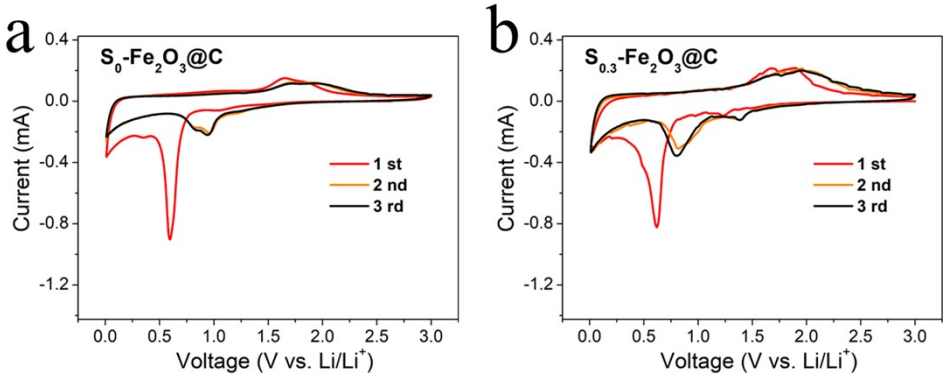

Figure S8. The first three CV curves at 0.1 mV s^{-1} of (a) S_0-Fe_2O_3@C and (b) $S_{0.3}$-Fe_2O_3@C electrodes

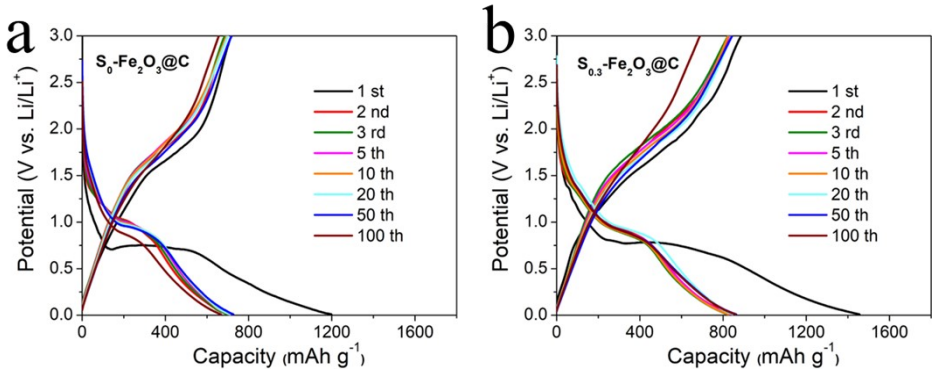

Figure S9. Galvanostatic discharge-charge profiles of (a) S_0-Fe_2O_3@C and $S_{0.3}$-Fe_2O_3@C electrodes at 200 mA g^{-1}.

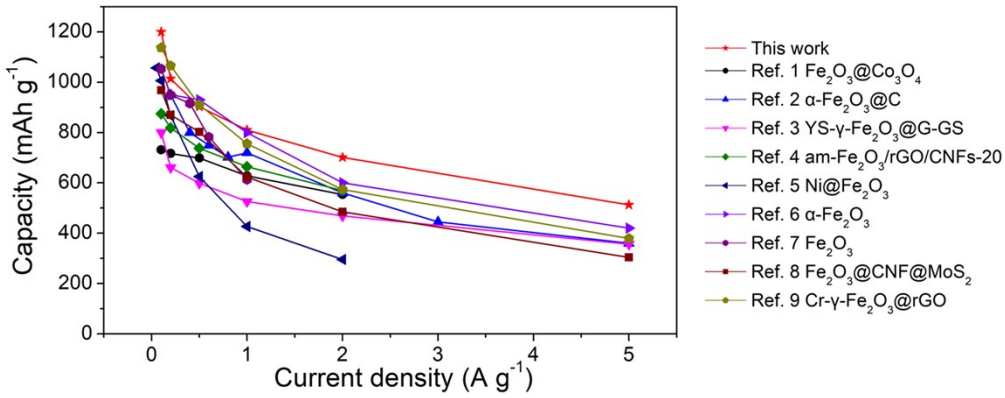

Figure S10. Comparison of rate capabilities of $S_{0.15}$-Fe_2O_3@C electrode and other reported Fe_2O_3-based LIB anode materials.

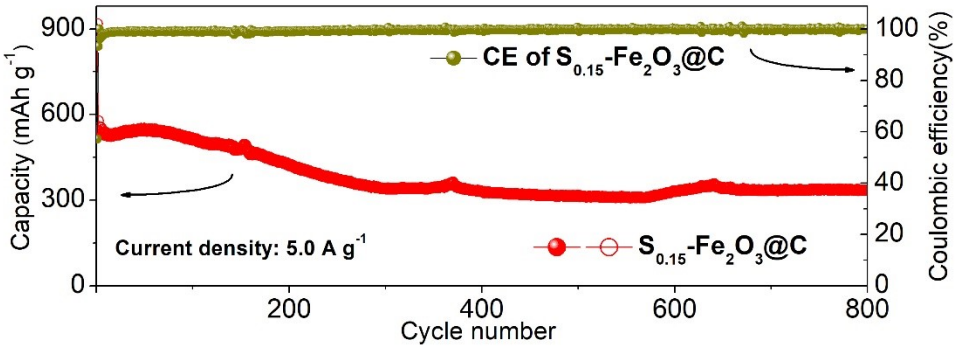

Figure S11. Cycle performance of $S_{0.15}$-Fe_2O_3@C electrode at 5.0 A g^{-1}.

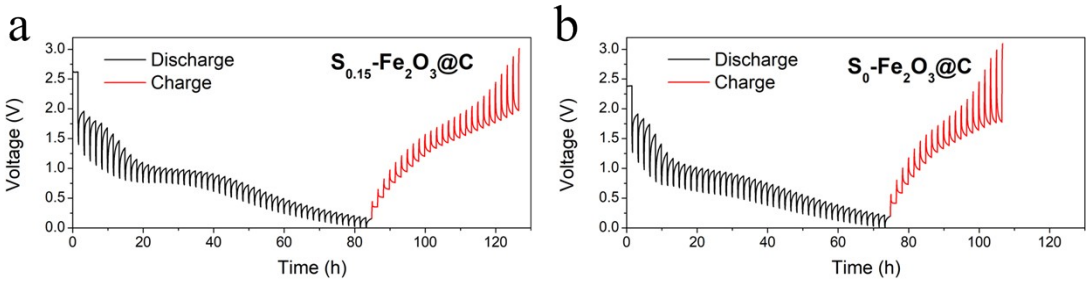

Figure S12. Discharge/charge state curves of GITT patterns for $S_{0.15}$-Fe_2O_3@C and S_0-Fe_2O_3@C electrodes at 200 mA g^{-1}

The Li-ion diffusion coefficients of $S_{0.15}$-Fe_2O_3@C and S_0-Fe_2O_3@C electrodes can be measured according to the following Equation (1)

$$D_{Li^+} = \frac{4L^2}{\pi\tau}\left(\frac{\Delta E_S}{\Delta E_\tau}\right)^2 \quad (1)$$

where L and τ are the thickness of the electrodes (cm) and the duration of the current pulse (s), respectively. ΔE_s is the change in steady-state voltage (V) for a single-step GITT measurement, and ΔE_τ is the voltage change (V) during one discharge pulse regardless of IR drop.

Table S1. The XPS composition analysis (O, S, Fe, C) of $S_{0.15}$-Fe_2O_3@C and $S_{0.3}$-Fe_2O_3@C.

samples	O (at. %)	S (at. %)	Fe (at. %)	C (at. %)
$S_{0.15}$-Fe_2O_3@C	11.03	1.57	1.91	85.49
$S_{0.3}$-Fe_2O_3@C	9.03	2.17	1.87	86.93

(1). Zhang, S. L.; Guan, B. Y.; Wu, H. B.; Lou, X. W. D. Metal–Organic Framework-Assisted Synthesis of Compact Fe_2O_3 Nanotubes in Co_3O_4 Host with Enhanced Lithium Storage Properties. *Nano-Micro Letters* **2018,** *10*, 44.

(2). Wang, Y.; Guo, X.; Wang, Z.; Lü, M.; Wu, B.; Wang, Y.; Yan, C.; Yuan, A.; Yang, H. Controlled pyrolysis of MIL-88A to Fe_2O_3@C nanocomposites with varied morphologies and phases for advanced lithium storage. *J. Mater. Chem. A,* **2017,** *5*, 25562-25573.

(3). Zhang, M.; Liu, E.; Cao, T.; Wang, H.; Shi, C.; Li, J.; He, C.; He, F.; Ma, L.; Zhao, N. Sandwiched graphene inserted with graphene-encapsulated yolk–shell γ-Fe_2O_3 nanoparticles for efficient lithium ion storage. *J. Mater. Chem. A,* **2017,** *5*, 7035-7042.

(4). Zhao, Q.; Liu, J.; Li, X.; Xia, Z.; Zhang, Q.; Zhou, M.; Tian, W.; Wang, M.; Hu, H.; Li, Z.; Wu, W.; Ning, H.; Wu, M. Graphene oxide-induced synthesis of button-shaped amorphous Fe_2O_3/rGO/CNFs films as flexible anode for high-performance lithium-ion batteries. *Chem. Eng. J.* **2019,** *369*, 215-222.

(5). Backert, G.; Oschmann, B.; Tahir, M. N.; Mueller, F.; Lieberwirth, I.; Balke, B.; Tremel, W.; Passerini, S.; Zentel, R. Facile hybridization of Ni@Fe_2O_3 superparticles with functionalized reduced graphene oxide and its application as anode material in lithium-ion batteries. *J. Colloid Interface Sci.* **2016,** *478*, 155-63.

(6). Yang, S.; Zhou, B.; Ding, Z.; Zheng, H.; Huang, L.; Pan, J.; Wu, W.; Zhang, H. Tetragonal hematite single crystals as anode materials for high performance lithium ion batteries. *J. Power Sources* **2015,** *286*, 124-129.

(7). Sun, M.; Sun, M.; Yang, H.; Song, W.; Nie, Y.; Sun, S. Porous Fe_2O_3 nanotubes as advanced anode for high performance lithium ion batteries. *Ceram. Int.* **2017,** *43*, 363-367.

(8). Huang, X.; Cai, X.; Xu, D.; Chen, W.; Wang, S.; Zhou, W.; Meng, Y.; Fang, Y.; Yu, X. Hierarchical Fe_2O_3@CNF fabric decorated with MoS_2 nanosheets as a robust anode for flexible lithium-ion batteries exhibiting ultrahigh areal capacity. *J. Mater. Chem. A,* **2018,** *6*, 16890-16899.

(9). Pan, X.; Duan, X.; Lin, X.; Zong, F.; Tong, X.; Li, Q.; Wang, T. Rapid synthesis of Cr-doped γ-Fe_2O_3/reduced graphene oxide nanocomposites as high performance anode materials for lithium ion batteries. *J. Alloys Compd.* **2018,** *732*, 270-279.